Molecular BioSystems

Accepted Manuscript

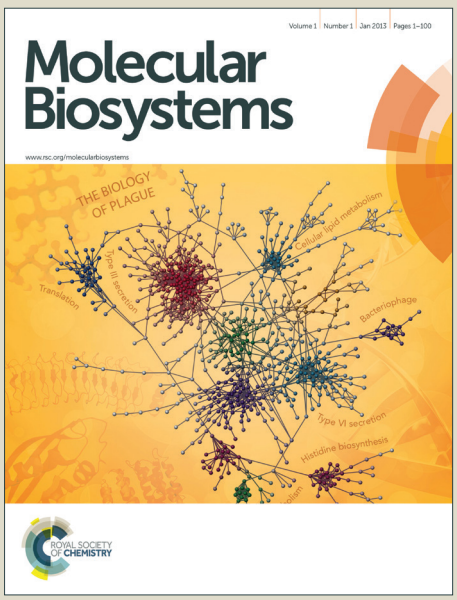

ROYAL SOCIETY OF CHEMISTRY

www.rsc.org/molecularbiosystems

The hydrolyzable gallotannin, penta-*O*-galloyl-*β*-D-glucopyranoside, inhibits the formation of advanced glycation endproducts by protecting protein structure

Hang Ma [1a], Weixi Liu [2a], Leslie Frost [3], Ling Wang [4], Liwen Kong [1], Joel A. Dain[2*], Navindra P. Seeram [1*]

[1]*Bioactive Botanical Research Laboratory, Department of Biomedical and Pharmaceutical Sciences, University of Rhode Island, Kingston, RI, 02881, USA*
[2]*Department of Chemistry, University of Rhode Island, Kingston, RI, 02881, USA*
[3]*Department of Chemistry, Marshall University, Huntington, WV, 25755, USA*
[4]*School of Bioscience and Bioengineering, South China University of Technology, Guangzhou, 510006, China*

[a] These authors contributed equally to this work

* Corresponding authors

***Navindra P. Seeram**
7 Greenhouse Road
Kingston, RI, United States
Fax: + (1) 401 874 5787
Phone: + (1) 401 874 9367
Email: nseeram@uri.edu

***Joel A. Dain**
51 Lower College Road
Kingston, RI, United States
Fax: + (1) 401 874 5072
Phone: + (1) 401 874 5942
Email: jdain@chm.uri.edu

Graphic Abstract

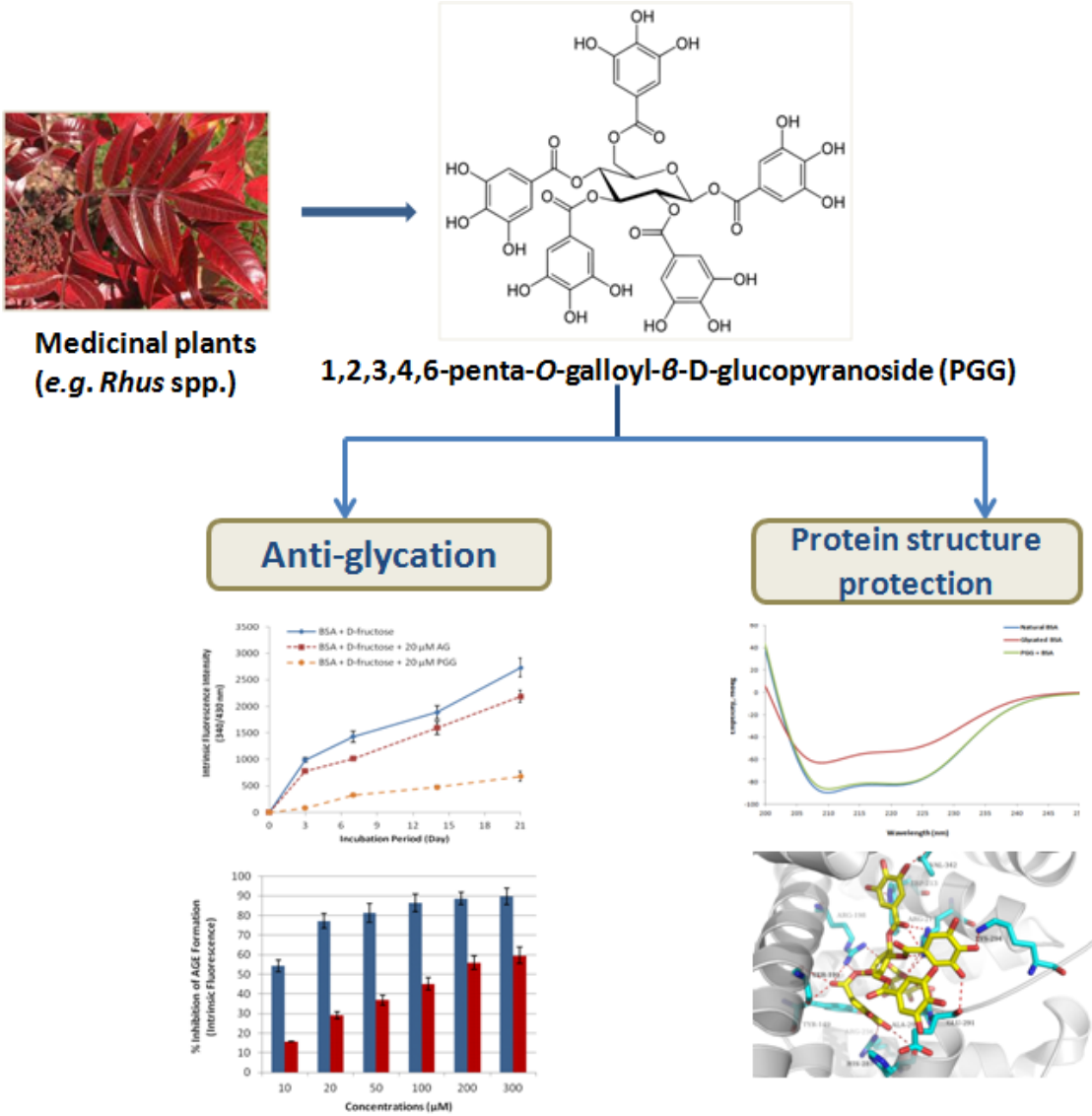

The prototypical hydrolyzable tannin, pentagalloylglucose (PGG), inhibits formation of AGEs at all stages of glycation and protects protein structure.

Abstract

Glycation is a spontaneous process initiated by a condensation reaction between reducing sugars and proteins that leads to the formation of Advanced Glycation Endproducts (AGEs). The *in vivo* accumulation of AGEs is associated with several chronic human diseases and, thus, the search for AGE inhibitors is of great research interest. Hydrolyzable tannins (gallotannins and ellagitannins) are bioactive plant polyphenols which show promise as natural inhibitors of glycation and AGE formation. Notably, the gallotannin, 1, 2, 3, 4, 6-penta-*O*-galloyl-*β*-D-glucose (PGG), is a key intermediate involved in the biosynthesis of hydrolyzable tannins in plants. Herein, we investigated the effects of PGG on the individual stages of protein glycation and on protein structure (using Bovine Serum Albumin; BSA). MALDI-TOF data demonstrated that PGG inhibited early glycation by 75% while the synthetic AGE inhibitor, aminoguanidine (AG), was not active (both at 50 μM). In addition, PGG reduced the formation of middle and late stage AGEs by 90.1 and 60.5%, respectively, which was superior to the positive control, AG. While glycation induced conformational changes in BSA from α-helix to β-sheets (from circular dichroism and congo red binding studies), PGG (at 50 μM) reduced this transition by 50%. Moreover, BSA treated with PGG was more stable in its structure and retained its biophysical properties (based on zeta potential and electrophoretic mobility measurements). The interaction between PGG and BSA was further supported by molecular docking studies. Overall, the current study adds to the growing body of data supporting the anti-AGE effects of hydrolyzable tannins, a ubiquitous class of bioactive plant polyphenols.

1 INTRODUCTION

Hydrolyzable tannins, constituting gallotannins and ellagitannins, are bioactive polyphenols which are abundant in fruit, berries, medicinal plants, and their derived products. Notably, the gallotannin, 1, 2, 3, 4, 6-penta-*O*-galloyl-*β*-D-glucose (PGG; chemical structure shown in Figure 1), is a key intermediate and immediate precursor involved in the biosynthesis of hydrolyzable tannins in terrestrial plants.[1-3] PGG is biosynthesized from gallic acid and glucose by UDP-glucose enzyme catalyzed series of position-specific galloylation steps. Initially, β-glucogallin (1-*O*-galloyl-*β*-D-glucose) is formed and subsequent esterification steps, with extreme position specificity, yields the metabolic formation sequence of 1,6-digalloylglucose followed by 1,2,6-trigalloylglucose, 1,2,3,6-tetragalloylglucose, and finally, PGG.[3] Further galloylation of PGG generates other gallotannins (such as hexa-, hepta- and octa-galloylglucoses with *meta*-depside bonds) while ellagitannins are produced via a series of intra- and/or inter-molecular oxidative crosslinking between galloyl units. Given, its ubiquity, abundance, and central role as a biosynthetic precursor of hydrolyzable tannins in plants, PGG has been extensively studied for a variety of biological effects, including anticancer and antidiabetic properties, in both *in vitro* [3-5] and preclinical animal models.[3, 6, 7] Interestingly, PGG has been shown to inhibit alpha-glucosidase enzyme activity and act as an insulin mimetic [8] as well as reduce high fat induced diabetes in mice.[9]

Advance glycation endproducts (AGEs) are a polymorphic group of compounds formed initially from a reversible condensation reaction between carbonyl groups of reducing sugars

and amino groups of proteins, *i.e.* lysines, arginines and cysteines.[10] The products of this initial stage, namely Schiff bases, are then converted to more stable aldimine structures referred to as Amadori products. In the advanced stage of glycation, Schiff bases and Amadori products undergo various types of chemical changes such as dehydration, oxidation, and rearrangements ultimately leading to the formation of AGEs.[10,11] The formation and accumulation of AGEs *in vivo* has been linked with several chronic human diseases including diabetes, atherosclerosis, and Alzheimer's disease.[12-14]

Proteins with a longer half-life are particularly vulnerable to modifications to form protein-AGE adducts. Indeed, many of these modified proteins have been identified *in vivo, e.g.* albumin, hemoglobin, collagen, and fibrinogen.[10, 15, 16] Under hyperglycemic conditions, AGE formation is significantly accelerated, resulting in undesirable accumulation of modified proteins in circulation and cells.[17,18] Protein-AGE adducts are associated with many progressive complications of diseases such as diabetes and have been shown to be toxic to diverse cell types including retinal capillary cells, endothelial cells, and neuronal cells.[19-21] To date, several mechanisms have been proposed to explain the deleterious effects of AGEs. For instance, intracellular AGEs up-regulate oxidative stress and inflammation by binding to cell membrane proteins such as Receptor for AGEs (RAGE), AGE Receptor Complex (AGE-RG), and macrophage scavenger receptor.[13,22] Moreover, extracellular accumulation of AGEs can cause crosslinks on long lived proteins and protein aggregation,

which consequentially leads to alteration in protein structures and impairment of their functions.[10, 23]

Given that the *in vivo* formation and accumulation of AGEs play a significant role in the pathophysiology of several chronic human diseases, there has been an ongoing research effort to discover synthetic and natural inhibitors of these processes.[24, 25] While several synthetic compounds show strong anti-glycation activities, many including metformin, pyridoxyamine, and aminoguanidine (AG) have been shown to have severe side effects in clinical studies.[24, 26] However, natural compounds, including plant-derived polyphenols found in medicinal plants and plant foods, have shown great promise as alternative dietary strategies to prevent AGE related diseases.[25, 27]

Our group has been involved in a program of studies to isolate, identify, and elucidate the mechanisms of actions of hydrolyzable tannins, namely, gallotannins and ellagitannins, from medicinal plants targeting diabetes and Alzheimer's disease.[28, 29] We have recently reported on the anti-AGE effects of ellagitannins from the pomegranate fruit,[30] and were interested in whether similar effects/mechanisms of actions would be exerted by gallotannins, namely, PGG, given its central role as a biosynthetic precursor of hydrolyzable tannins in plants. While PGG and several of its closely related natural analogs have been reported to inhibit protein glycation,[31] the mechanisms of these actions are still unclear. Also, since hydrolyzable tannins are known to bind extensively to proteins,[32-34] we investigated whether

PGG would exert protective effects on protein structure during glycation using bovine serum albumin (BSA). BSA was selected as the 'model protein' because it is a well-characterized protein which has been used extensively in published studies involving tannin-protein interactions.[34] This is the first report to examine the effects of PGG on the different stages of glycation (initial, middle, and final) as well as its protective effects on protein structure.

2 EXPERIMENTAL

2.1. General Experimental

Bovine serum albumin (BSA), D-fructose, aminoguanidine hydrochloride (AG), and sinapic acid were purchased from Sigma-Aldrich Chemical Co. (St. Louis, MO, USA). Congo red, HPLC-grade acetonitrile and trifluoroacetic acid (TFA) were obtained from Thermo Fisher Scientific (Rockford, IL, USA). ZipTip pipette tips with C_4 resin and 0.22 µm filter units were purchased from EMD Millipore Co. (Billerica, MA, USA). G.K. peptide was obtained from Bachem Americas, Inc. (Torrance, CA, USA).

^{1}H and ^{13}C nuclear magnetic resonance (NMR) spectra were obtained on a Bruker 400 MHz spectrometer. Deuterated methanol (methanol-d_4) was used as solvent. Electrospray ionization mass spectra (ESIMS) data were obtained on a Q-Star Elite (Applied Biosystems MDS) mass spectrometer equipped with a Turbo Ionspray source and were acquired by direct infusion of pure compounds.

Analytical high-performance liquid chromatography (HPLC) was carried out on a Hitachi Elite LaChrom system consisting of an L-2130 pump, an L-2200 autosampler, an L-2455 diode array detector (DAD) and an L-2485 programmable fluorescence (FL) detector all operated by EZChrom Elite software (Pleasanton, CA, USA). All HPLC solvents were obtained from Wilkem Scientific (Pawcatuck, RI, USA).

2.2. Isolation and Identification of Pentagalloyl Glucose (PGG)

Our group has previously reported on the isolation and structure elucidation of compounds from the fruits of *Rhus copallinum* L. species (commonly known as winged sumac).[35] For the current project, PGG was isolated from the leaves of this plant species. Briefly, *R. copallinum* leaves (164.5 g) was macerated in methanol (2 × 400 mL × 12 h) to offer a dried methanol extract (90.5 g) after solvent removal *in vacuo*. The methanol extract (90.0 g) was subjected to a sequential liquid-liquid partitioning with *n*-hexanes (3 × 400 mL), ethyl acetate (3 × 400 mL) and *n*-butanol (3 × 400 mL) to yield *n*-hexanes (17.2 g), ethyl acetate (38.4 g) and *n*-butanol (22.5 g) extracts, respectively. The *n*-butanol extract (22.0 g) was further reconstituted in 50% aqueous methanol and adsorbed onto an Amberlite XAD-16 resin column (45 x 3 cm) which was eluted with a gradient solvent system consisting of water and methanol (from 100:0 to 10:90, v/v) to afford fourteen sub-fractions (Fr1-14). Fraction 2 (1.3 g) was further purified by semi-preparative HPLC to afford PGG (50.7 mg). The chemical structure of PGG was confirmed on the basis of the ^{1}H and ^{13}C NMR and mass spectral data and by comparison of these to published literature reports.[33, 36]

2.3. Characterization of Early Stage Glycation: BSA-Fructose MALDI-TOF Spectrum

The formation of early glycation and Amadori products was characterized using previously reported methods.[30,37] Briefly, 10 mg/mL BSA and 100 mM D-fructose were mixed and incubated in the presence or absence of 50 µM PGG in 0.1 M phosphate buffer, pH 7.4. Blank solutions included either BSA alone (10 mg/mL) or D-fructose alone (100 mM). The positive control solution contained 10 mg/mL BSA, 100 mM D-fructose, and 50 µM aminoguanidine (AG). D-fructose was chosen as the model glycating agent due to its higher reactivity compared to D-glucose. Moreover, D-fructose can be formed *in vivo* and the AGEs generated from fructose-induced glycation, i.e. fructosylation, have been shown to play an important role in the pathogenesis of several diseases.[38] Unless otherwise indicated, all of the reaction mixtures were prepared in triplicate and incubated at 37 °C in the dark for 24 hours. Albumin protein samples were analyzed on a Bruker Autoflex MALDI-TOF mass spectrometer (Bruker Daltonics Inc., Billerica, MA, USA) with instrument settings optimized for intact protein analyses using a delayed extraction of 60 nanoseconds. Prior to analyses, the proteins were purified using C4 ZipTips and mixed with a saturated solution of α-cyano-4-hydroxy-cinnamic acid containing 0.05 % TFA. The mass spectra were recorded in positive ion mode in the m/z range from 20,000 to 80,000. Typically, 3000 spectra were accumulated with 50 laser shots for each sample spot analyzed. FlexAnalysis and ClinProTools software (Bruker Daltonics Inc., Billerica, MA, USA) were used for the analyses of the data.

2.4. Characterization of Middle Stage Glycation

2.4.1. BSA-Fructose Intrinsic Fluorescence

All solutions were prepared in 0.1 M phosphate buffer, pH 7.4, under sterilized condition. The final concentrations of BSA and D-fructose in each reaction mixtures were adjusted to 10 mg/mL and 100 mM, respectively. BSA-fructose mixtures were then incubated in the absence or presence of different concentrations of PGG ranging from 10 to 300 µM. BSA alone (10 mg/mL), D-fructose alone (100 mM), or PGG alone (10, 20, 50, 100, 200 and 300 µM) served as blank solutions. The positive control contained 10 mg/mL BSA, 100 mM D-fructose, and different concentrations of AG (10, 20, 50, 100, 200 and 300 µM). All reaction mixtures were prepared in triplicate and incubated at 37 °C for up to 21 days. On day 0, 3, 7, 14 and 21, aliquots were collected from each incubation tube for a time course study. Prior to analyses, 50 µL of each sample was diluted with 150 µL 0.1 M phosphate buffer and then transferred to 96-well black fluorescence reading plates. Measurements of emission intensity at 430 nm were obtained from a Spectra Max M2 spectrometer (Molecular Devices, Sunnyvale, CA, USA). To determine the total AGE fluorescence, the excitation wavelength was set at 360 nm, according to previously reported methods. [39]

2.4.2. BSA-Fructose HPLC-FL Analyses

Reaction mixtures for HPLC-FL analyses included 10 mg/mL BSA and 100 mM D-fructose with or without PGG (20 µM) in 0.1 M phosphate buffer, pH 7.4. The positive control was AG at a similar concentration. Blank solutions included either BSA alone (10 mg/mL) or PGG

alone (20 µM). All mixtures were prepared under sterilized conditions and incubated at 37 °C for 7 days. All AGE species were separated on a Shodex (New York, NY, USA) RSpak C_{18} reverse phase HPLC column (5 µm×4.6 mm×150 mm) with a 415 Å pore size. The mobile phase A consisted of 99% water (0.1% TFA) and 1% acetonitrile (ACN). The mobile phase B included 5% water (0.1% TFA) and 95% ACN. A linear gradient from 20 to 60% of mobile phase B was applied at a constant flow rate of 1.0 mL/min over 25 minutes. The formation of AGEs was monitored using a programmable fluorescence (FL) detector with excitation and emission wavelengths set at 360 nm and 430 nm, respectively. Prior to analyses, all solvents were degassed and sonicated for 15 min and all samples were filtered by a 0.22 micron membrane.

2.5. Characterization of Late Stage Glycation: G.K. Peptide Assay

G.K. peptide-ribose assay was performed to evaluate the formation of peptide cross-linking structures produced in the late stage of glycation as described previously.[40] Briefly, 40 mg/mL G.K. peptide was incubated with 100 mM D-ribose in 0.1 M phosphate buffer, pH 7.4 at 37 °C. Different amounts of PGG or positive control, AG, were added to G.K. peptide-ribose mixtures with their final concentrations adjusted to 1, 10, 50, 100 and 300 µM. After incubation for 6 hours, the fluorescence of each sample was obtained using a Spectra Max M2 spectrometer (Molecular Devices, Sunnyvale, CA, USA) at excitation and emission wavelengths of 340 and 420 nm, respectively.

2.6. Circular Dichroism (CD) Analyses

To evaluate the protective effect of PGG on protein secondary structure, CD analyses was performed with a Jasco J-720 spectropolarimeter (Tokyo, Japan). Analyzed sample mixtures included 10 mg/mL natural BSA, 10 mg/mL BSA glycated with 100 mM D-fructose (BSA-fructose mixture), BSA-fructose mixtures treated with 50 µM PGG or with 50 µM AG (positive control). All of the above mixtures were prepared in 0.1 M phosphate buffer, pH 7.4, in triplicate and incubated in dark at 37 °C for 7 days. Prior to spectral acquisition, the concentration of BSA in each sample was adjusted to 1 mg/mL with the 0.1 M phosphate buffer, pH 7.4. CD spectral signatures were obtained in the far-ultraviolet region (190-260 nm) with bandwidth set to 1 nm and 10 repetitive scans were performed for each sample. The percentages of BSA's secondary structure composition were estimated with Selcon 3 method [41] using DichroWeb program. [42]

2.7. Congo Red Binding Assay

The congo red binding assay was carried out according to previously reported methods[16] with minor modifications. Briefly, 100 µM congo red was freshly prepared in PBS with 10% (v/v) ethanol. 70 µL congo red solution was then mixed with 80 µL protein sample and 320 µL PBS, resulting in a final protein concentration of 25.0 µM in each sample. Absorbance scans from 480 to 560 nm were obtained using an UltroSpec 2100 instrument (Biochrom Ltd, Cambridge, UK) with congo red solution alone serving as the background. The following samples were evaluated for their binding ability with congo red dye and each sample was

prepared in triplicate: 1) natural BSA, 2) BSA-fructose mixture, 3) BSA-fructose mixture treated with 100 µM PGG, and 4) BSA-fructose mixture treated with 100 µM AG. All mixtures were prepared in 0.1 M phosphate buffer, pH 7.4 under sterilized condition and incubated in dark at 37 °C for 21 days.

2.8. BSA Zeta Potential Measurement

The zeta potential and the electrophoretic mobility of each sample were measured with a Zetasizer Nano-ZS90 (Malvern, Worcestershire, UK) using laser doppler micro-electrophoresis technique. For this purpose, four sets of samples, each in triplicate, were prepared in PBS buffer, pH 7.4, and incubated in the dark at 37 °C for 7 days prior to analyses: 1) 10 mg/mL natural BSA, 2) 10 mg/mL BSA with 100 mM D-Fructose (BSA-Frc mixture), 3) BSA-Frc mixture treated with 100 µM PGG, and 4) BSA-Frc mixture treated with 100 µM AG. The operating temperature was set at 25 °C and 100 consecutive runs were obtained for each sample.

2.9. Molecular Docking Studies

For the molecular docking study, the initial structure of BSA was obtained from the Protein Data Bank (PDB ID: 4F5S).[43] Two potential ligand binding sites, namely, the substrate binding site and the Trp213 binding site were defined as in previous studies.[44-46] PGG was optimized using MMFF94s force field, and then the protein structure was protonated based on AMBER-99 force field after removing water molecules. MOE-docking (MOE 2010.10,

Chemical Computing Group, Inc., Montreal, Canada) was employed to identify the binding poses of PGG and BSA. All docked poses of PGG were ranked on the basis of the binding docking energies. The lowest energy conformation was chosen for binding modes analyses.

3 Results

3.1. Effects of PGG on Early Stage Glycation

Figure 2 shows the MALDI-TOF mass spectral profiles of doubly charged BSA in: 1) blank solution containing BSA alone (black line), 2) glycated BSA without any treatment (green line), glycated BSA treated with 50 µM PGG (blue line), and 4) glycated BSA treated with 50 µM AG serving as the positive control (red line). The increase in the mass of BSA after its glycation with D-fructose was due to the condensation of the sugar molecules with the protein during early stage glycation.[47] A greater extent of glycation results in a higher mass shift compared to the molar mass of natural BSA and the number of sugar adducts on each protein molecule can be calculated based on such shifts using the following equation: number of sugar adducts = (m/z of glycated protein – m/z of natural protein) X z/molar mass of sugar.

Analyses of the data showed that the most pronounced shifts in the m/z value of BSA occurred in the control solution that contained only BSA and D-fructose without any treatments. Native BSA exhibited an m/z value at 33180 whereas that of the control yielded an m/z value of 33540. It should be noted that all m/z values presented here were obtained

from doubly charged BSA (z = 2). This difference in the m/z values represented the condensation of 4 sugar residues onto the protein. In the case of the reaction mixture containing 50 µM PGG, the changes in the m/z value were less pronounced compared to the control solution, generating a protein peak with an m/z of 33260. Thus, relative to native BSA, this represented only 1 D-fructose adduct. However, the positive control, AG (also at 50 µM) generated a MALDI-TOF spectrum similar to that of the control, indicating that AG exhibited none or a minimal effect on early stage glycation. In contrast, PGG inhibited the formation of early glycation products by 75%. In summary, in the PGG treated samples, only 1 sugar adduct was condensed with BSA, while in the control or AG treated solutions, 4 sugar molecules were found to be glycated with BSA within 24 hours of reaction.

3.2. Effects of PGG on Middle Stage Glycation

3.2.1. Intrinsic Fluorescence

The effect of PGG on middle stage glycation was then evaluated by intrinsic fluorescence and HPLC-FL. In this phase of reaction, Schiff bases or Amadori products generated from early glycation can degrade and release reactive dicarbonyl compounds.[10, 11] Such species react with proteins or early glycation products at a much higher rate to produce crosslinking structures which exhibit characteristic fluorescence. The excitation wavelength of 360 nm and an emission wavelength of 430 nm have been previously reported as optimum for detecting total fluorescent AGEs of BSA and other proteins.[39]

The intrinsic fluorescence profiles showed that there were increases in the fluorescent intensity of all of the incubation mixtures that contained BSA and D-ribose, regardless, of whether PGG or AG were included in the reaction mixtures or not. Blank solutions containing BSA alone or D-fructose alone yielded no increases in fluorescent readings (data not shown). Figure 3 A displays the time course profiles of the control solution containing BSA and D-fructose only, BSA-fructose mixture treated with 20 μM PGG, and BSA-fructose mixture treated with 20 μM AG. The fluorescent profiles showed that fluorescent intensities increased over time from day 0 to day 21 for all of the three samples. Glycation is a time-dependent process and therefore this increase in fluorescence is expected.[47] Fluorescent readings were highest in samples that contained only BSA and D-ribose during the entire incubation process. AG and PGG both showed inhibitory effects on the formation of crosslinking fluorescent AGEs throughout the entire incubation period, yielding fluorescent readings lower than that of control. Moreover, PGG treated samples also showed a reduced glycation rate as compared to the control solutions and AG treated samples (see Figure 3 A).

Based on the intrinsic fluorescent intensities, the percent inhibition of AGE formation was calculated using the following equation: % inhibition = [1-(fluorescence intensity of solution with inhibitor/fluorescence intensity of control solution)] x 100%. Figure 3 B shows the percent inhibition of different concentrations of PGG and AG after 7 days of incubation.

PGG reduced AGE formation by more than 50% while the positive control, AG, only showed 16% inhibition at an equivalent concentration of 10 µM.

3.2.2. HPLC-FL Data

Figure 4 displays the HPLC-FL profiles of the control solution without any treatment (4 A), reaction mixture treated with 20 µM AG (4 B), or with 20 µM PGG (4 C). In each of the profiles, peaks I, II, and III with retention times (R_t) of 10.74, 11.38 and 20.13 min, respectively, represented the fluorescent AGE products of BSA detectable at excitation and emission wavelengths of 360 nm and 430 nm, respectively. Repeated HPLC-FL analyses showed that these peaks occurred routinely in all of the mixtures containing BSA and D-fructose. The HPLC-FL profile of the blank solution containing BSA alone yielded no fluorescence peaks (data not shown).

Examination of the integrated areas under peaks I, II, and III for each sample revealed that glycation products were most pronounced in the control that contained only BSA and D-fructose, which was in agreement with the intrinsic fluorescence data. The HPLC-FL profile of the control solution yielded three AGE peaks with a total peak area set to 100 %. In comparison, the formation of fluorescent AGEs was less pronounced in mixtures treated with AG or PGG, yielding total AGE peak areas of 68.7 and 27.7 %, respectively. Based on the peak areas of fluorescent AGEs, the positive control, AG, reduced the formation of glycation

products by 31.3% while in the PGG treated sample, AGE formation was decreased by 72.3%, indicating that PGG is a more potent inhibitor on middle stage glycation than AG.

3.3. Effects of PGG on Late Stage Glycation

Dimerization of lysine containing peptide and advanced Maillard reaction products can be formed through lysine-lysine cross linking to further generate late stage AGEs. The preventive effects of PGG on the formation of cross-linked final glycation products can be characterized by the G.K. peptide-ribose assay. In this assay, the formation of protein cross-linking products was inhibited by PGG in a concentration dependent manner. As shown in Figure 5, PGG effectively inhibited (by 60.5 %) the formation of late stage AGEs in a concentration dependent manner while AG showed weaker inhibitory effects (of 17.2 %) at an equivalent concentration of 300 μM.

3.4. Protective Effects of PGG on Protein Structure

3.4.1. CD Analyses

Glycation and AGE formation can change the biochemical and biophysical properties of proteins in several ways. While glycation occurs, sugar molecules covalently bind to certain amino acid residues on proteins and cause alteration of their secondary structures[16] and such changes can be monitored by a CD spectropolarimeter at the far-UV region (190-250 nm). Therefore, to evaluate the effect of PGG on the conformational change of glycated BSA, CD scans were performed at this region on reaction mixtures of: 1) native BSA serving

as the blank, 2) control solution containing BSA and D-fructose only, and 3) BSA and D-fructose incubated with PGG. Figure 6 displays the respective CD spectra of the above solutions and their conformational compositions (α helix and β strand) are summarized in Table I. Based on the quantitative analyses of the spectra, native BSA was composed of 57.5 % α-helix and 4.1 % β strands, which is in agreement with literature.[49] After glycation by D-fructose, BSA displayed a CD spectrum with similar features as that of native BSA, but with reduced signals at 208 nm and 222 nm. Such changes indicate a conformational change of the protein and the calculation of the secondary structural composition showed a significant decrease in α-helix content from 57.5 to 17.2 %, accompanied by an increase in β-strand formation from 4.1 to 24.2 %. However, in the PGG treated sample, the secondary structure of BSA was stabilized and a much smaller change in its secondary structure was observed. The α-helix content of BSA, in this case, increased to 35.8 % while the β strands content decreased to 11.3 % compared to untreated samples. The positive control, AG, also prevented the conformational change of BSA and showed similar but slightly weaker protective effects compared to PGG. The percent α-helix and β strands values in AG treated sample were 29.5 and 17.9 %, respectively.

3.4.2. Congo Red Binding Assay

Glycation of proteins can cause conformational transition from α-helix to β-strand which is the structural unit that forms β sheets. It is known that β sheets formation can perturb secondary structures of protein and accelerate protein aggregation.[16, 20] Such conformational

changes might cause a loss of protein functions and their physiological activities. Hence, we evaluated the protective effects of PGG against β sheet formation during glycation (by the congo red binding assay) using BSA-fructose mixture as the model system. Congo red is a dye previously shown to interact with cross-β structures in proteins and produces a characteristic absorption at 520-530 nm. Figure 7 shows the UV-Vis spectra of native BSA (blue), glycated BSA without any treatment (red), PGG treated BSA (green), and AG treated BSA (purple). All of the four spectra exhibited a λ_{max} of 520 nm with the minimal intensity observed in samples containing natural BSA. Glycated BSA without any treatment showed the most prominent enhancement in β sheet formation, yielding the highest reading at 520 nm. To better compare the data, the intensities of all samples at 520 nm were normalized based on the readings of the blank solutions and negative control solutions which were adjusted to 0 and 100%, respectively. A noticeable decrease of UV-Vis intensities were observed in samples treated with either PGG or AG (both at 100 μM) yielding normalized values of 38.3 and 43.3%, respectively. This represented a 61.7% decrease in β sheet formation in protein solutions containing PGG while a slightly lower inhibition (56.7%) was observed with AG.

3.4.3. Zeta Potential Measurement

Proteins structurally modified by glycation show alterations in their biophysical properties such as isoelectric point, electrophoretic mobility, and surface hydrophobicity.[44, 50] Since PGG showed protective effects on the secondary structure of BSA and prevented its

conformational changes, we evaluated the effects of PGG on these biophysical parameters using Zetasizer.

Lysine and arginine residues are two major glycation sites of proteins, which are both positively charged under physiological conditions. When glycation occurs, these residues are modified and neutralized by reducing sugars, resulting in an increase in the negative charges and a decrease in the isoelectric points of proteins.[50, 51] Moreover, the surface hydrophobicity of glycated proteins is generally higher than that of their native forms due to conformational alterations and partial unfolding.[51] The changes in the isoelectric points of proteins can be quantified by zeta potential measurement while the changes in surface hydrophobicity can be detected by monitoring electrophoretic mobility.

As shown in Table II, at pH 7.4, glycated BSA exhibited a much higher zeta potential value compared to natural BSA (-106.3 versus -8.18 mV) which is in agreement with previously reported data.[44] However, BSA samples co-incubated with PGG showed an average zeta potential reading of -30.9 mV, which was significantly reduced compared to untreated BSA. Glycated BSA without any treatment also displayed a noticeable increase in its electrophoretic mobility while the PGG treated BSA samples exhibited a mobility level closer to that of native BSA. The positive control, AG, yielded zeta potential value and electrophoretic mobility levels similar to PGG, indicating that both PGG and AG had some protective effects on protein structure.

3.4.4. Binding modes of PGG and BSA

The binding modes of PGG and BSA were obtained by molecular docking studies. The crystal structure of BSA has been well characterized (PDB ID: 4F5S).[43] It is known that BSA consists of three domains (I, II, and III) and each domain can be divided into two subdomains “a” and “b”.[52] As shown in Figures 8 A and B, two potential binding sites of PGG to BSA were defined based on structural complementarities and previous studies.[44, 45] The first PGG binding site was located in subdomain Ib, which comprised of three helices and a loop structures. As shown in Figure 8 C, the phenolic hydroxyl groups of PGG can form four hydrogen bonds with the residues LYS-524, ASP-555, and VAL-546, respectively. The carbonyl group of PGG also forms a hydrogen bond with the residue ASN-404. In addition, the aromatic ring of PGG forms π-π stacking interactions with the side chain of residue PHE-550. All of these interactions can provide the binding energy to stabilize the PGG-BSA complex. This binding mode of PGG and BSA is similar to that reported for other natural products for instance, limonene and BSA. [44]

The second likely PGG binding site is located in the subdomain IIa of BSA (Figure 8 D). This binding site of BSA is comprised of the residues TRP-213, VAL-342, SER-191, ARG-256, HIS-287, TYR-149, ALA-290, GLU-291, LYS-294, ARG-217, and GLN-195. Similarly, as in the first binding site, the carbonyl or phenolic groups of PGG were also able to form hydrogen bonds with various amino acids residues in this binding site. Thus it can be

concluded that PGG mainly interacted with BSA via hydrogen bonds thereby increasing the stability of the PGG-BSA complex.

4. Discussion and Conclusion

In this study, we have shown that the naturally occurring hydrolyzable gallotannin, PGG, inhibits all of the stages of glycation superior to the synthetic compound, AG. Notably, AG has been reported to be a strong carbonyl scavenger [26] and it inhibits the formation of AGEs by competitively binding to reactive carbonyl species such as methylglyoxal, the precursor of AGEs. Recently, our group reported that ellagitannins also inhibited the formation of AGEs by trapping reactive carbonyl species.[30] Interestingly, the gallotannin studied here, namely PGG, also showed promising anti-glycation activity, but without the similar scavenging effect on reactive carbonyl species (data not shown). Therefore, while it appears as if different mechanisms of anti-glycation effects are displayed by these two sub-classes of hydrolyzable tannins, namely, gallotannins and ellagitannins, further studies to elucidate the role of the chemical/structural differences of these two sub-classes are warranted.

Ellagitannins have been shown to bind weakly to proteins with compact globular tertiary structures unlike gallotannins which have a much stronger binding affinity with these proteins.[34] Therefore, we hypothesized that proteins treated with PGG might be more stabilized and less vulnerable to glycation due to PGG's binding ability with such proteins. Using BSA as a model protein, we showed that PGG reduced glycation levels at all of the

stages of the reaction and also prevented conformational changes of the protein. In addition, less formation of β sheets and a lower degree of protein unfolding were observed in the PGG treated samples indicating that PGG could maintain BSA's secondary structure and protect the protein from structural modification by glycation. Moreover, as displayed by the MALDI-TOF data, PGG inhibited the formation of early glycation and Amadori products while the positive control, AG, did not show any such activity. Therefore, this suggests that PGG binds to BSA at the initial stage of the reaction thereby stabilizing the protein's structure and preventing further modifications. Hence, PGG treated BSA was less susceptible to early glycation.

In conclusion, the natural polyphenolic compound, PGG, inhibited glycation at all stages of the reaction by protecting the secondary structure of proteins. This study lends support to the growing body of data supporting the anti-AGE effects of plant polyphenols, including hydrolyzable tannins, and warrants the further investigation of these natural compounds as alternative dietary strategies for the prevention and/or treatment of AGE related diseases including diabetes and Alzheimer's disease.

Acknowledgments

Data were acquired from instruments located at the University of Rhode Island in the RI-INBRE core facility obtained from Grant # P20RR016457 from the National Center for Research Resources (NCRR), a component of the National Institutes of Health (NIH). HM was supported by a graduate student scholarship from the Omar Magnate Family Foundation.

References

1. J. Cammann, K. Denzel, G. Schilling and G. G. Gross, *Archives of biochemistry and biophysics*, 1989, **273**, 58-63.
2. J. A. Ascacio-Valdés, J. J. Buenrostro-Figueroa, A. Aguilera-Carbo, A. Prado-Barragán, R. Rodríguez-Herrera and C. N. Aguilar, *Journal of Medicinal Plants Research*, 2011, **5**, 4696-4703.
3. J. Zhang, L. Li, S.-H. Kim, A. E. Hagerman and J. Lü, *Pharmaceutical research*, 2009, **26**, 2066-2080.
4. H. Hu, Y. Chai, L. Wang, J. Zhang, H. J. Lee, S.-H. Kim and J. Lü, *Molecular cancer therapeutics*, 2009, **8**, 2833-2843.
5. Y. Li, J. Kim, J. Li, F. Liu, X. Liu, K. Himmeldirk, Y. Ren, T. E. Wagner and X. Chen, *Biochemical and biophysical research communications*, 2005, **336**, 430-437.
6. J. Zhang, K. Nkhata, A. A Shaik, L. Wang, L. Li, Y. Zhang, L. A Higgins, K. H Kim, J. D Liao and C. Xing, *Current cancer drug targets*, 2011, **11**, 787-798.
7. Y. Cao, K. B. Himmeldirk, Y. Qian, Y. Ren, A. Malki and X. Chen, *Journal of natural medicines*, 2014, 1-8.
8. Y. Li, J. Kim, J. Li, F. Liu, X. Liu, K. Himmeldirk, Y. Ren, T. E. Wagner and X. Chen, *Biochem Biophys Res Commun*, 2005, **336**, 430-437.
9. C. Mohan, G. Viswanatha, G. Savinay, C. Rajendra and P. D. Halemani, *Phytomedicine*, 2013, **20**, 417-426.
10. R. Singh, A. Barden, T. Mori and L. Beilin, *Diabetologia*, 2001, **44**, 129-146.
11. R. Bucala and A. Cerami, *Advances in pharmacology*, 1992, **23**, 1-34.
12. H. Vlassara and M. Palace, *Journal of internal medicine*, 2002, **251**, 87-101.
13. V. Srikanth, A. Maczurek, T. Phan, M. Steele, B. Westcott, D. Juskiw and G. Münch, *Neurobiology of aging*, 2011, **32**, 763-777.
14. G. Basta, A. M. Schmidt and R. De Caterina, *Cardiovascular research*, 2004, **63**, 582-592.
15. D. H. Cribbs, B. Y. Azizeh, C. W. Cotman and F. M. LaFerla, *Biochemistry*, 2000, **39**, 5988-5994.
16. B. Bouma, L. M. Kroon-Batenburg, Y.-P. Wu, B. Brünjes, G. Posthuma, O. Kranenburg, P. G. de Groot, E. E. Voest and M. F. Gebbink, *Journal of biological chemistry*, 2003, **278**, 41810-41819.
17. E. Selvin, M. W. Steffes, H. Zhu, K. Matsushita, L. Wagenknecht, J. Pankow, J. Coresh and F. L. Brancati, *New England Journal of Medicine*, 2010, **362**, 800-811.
18. C. Loske, A. Neumann, A. Cunningham, K. Nichol, R. Schinzel, P. Riederer and G. Münch, *Journal of neural transmission*, 1998, **105**, 1005-1015.
19. R. Chibber, P. Molinatti, N. Rosatto, B. Lambourne and E. Kohner, *Diabetologia*, 1997, **40**, 156-164.
20. G. Münch, J. Thome, P. Foley, R. Schinzel and P. Riederer, *Brain research reviews*, 1997, **23**, 134-143.

21. M. Takeuchi, S. Kikuchi, N. Sasaki, T. Suzuki, T. Watai, M. Iwaki, R. Bucala and S.-i. Yamagishi, *Current Alzheimer Research*, 2004, **1**, 39-46.
22. S. F. Yan, R. Ramasamy and A. M. Schmidt, *Nature Reviews Endocrinology*, 2008, **4**, 285-293.
23. D. Aronson, *Journal of hypertension*, 2003, **21**, 3-12.
24. S. Rahbar and J. L. Figarola, *Archives of Biochemistry and Biophysics*, 2003, **419**, 63-79.
25. C.-H. Wu, S.-M. Huang, J.-A. Lin and G.-C. Yen, *Food & function*, 2011, **2**, 224-234.
26. P. J. Thornalley, *Archives of biochemistry and biophysics*, 2003, **419**, 31-40.
27. H. Y. Kim and K. Kim, *Journal of agricultural and food chemistry*, 2003, **51**, 1586-1591.
28. C. Wan, T. Yuan, L. Li, V. Kandhi, N. B. Cech, M. Xie and N. P. Seeram, *Bioorganic & medicinal chemistry letters*, 2012, **22**, 597-600.
29. A. H Ahmed, G. M Subaiea, A. Eid, L. Li, N. P Seeram and N. H Zawia, *Current Alzheimer Research*, 2014, **11**, 834-843.
30. W. Liu, H. Ma, L. Frost, T. Yuan, J. A. Dain and N. P. Seeram, *Food & function*, 2014, **5**, 2996-3004.
31. J. Lee, D. S. Jang, N. H. Kim, Y. M. Lee, J. Kim and J. S. Kim, *Biological and Pharmaceutical Bulletin*, 2011, **34**, 443-446.
32. G. Gyémánt, Á. Zajácz, B. Bécsi, C. Ragunath, N. Ramasubbu, F. Erdődi, G. Batta and L. Kandra, *Biochimica et Biophysica Acta (BBA)-Proteins and Proteomics*, 2009, **1794**, 291-296.
33. M. A. Dobreva, R. A. Frazier, I. Mueller-Harvey, L. A. Clifton, A. Gea and R. J. Green, *Biomacromolecules*, 2011, **12**, 710-715.
34. E. R. Deaville, R. J. Green, I. Mueller-Harvey, I. Willoughby and R. A. Frazier, *Journal of agricultural and food chemistry*, 2007, **55**, 4554-4561.
35. H. Ma, T. Yuan, A. Gonzalez-Sarrias, L. Li, M. E. Edmonds and N. P. Seeram, *Natural product communications*, 2012, **7**, 45-46.
36. G. Beretta, R. Artali, E. Caneva and R. Maffei Facino, *Magnetic Resonance in Chemistry*, 2011, **49**, 132-136.
37. L. Frost, M. Chaudhry, T. Bell and M. Cohenford, *Analytical biochemistry*, 2011, **410**, 248-256.
38. J. D. McPherson, B. H. Shilton and D. J. Walton, *Biochemistry*, 1988, **27**, 1901-1907.
39. A. Schmitt, J. Schmitt, G. Münch and J. Gasic-Milencovic, *Analytical biochemistry*, 2005, **338**, 201-215.
40. S. Rahbar, R. Natarajan, K. Yerneni, S. Scott, N. Gonzales and J. L. Nadler, *Clinica chimica acta*, 2000, **301**, 65-77.
41. N. Sreerama, S. Y. Venyaminov and R. W. Woody, *Protein Science*, 1999, **8**, 370-380.
42. L. Whitmore and B. A. Wallace, *Biopolymers*, 2008, **89**, 392-400.
43. A. Bujacz, *Acta Crystallographica Section D: Biological Crystallography*, 2012, **68**, 1278-1289.

44. M. M. Joglekar, S. N. Panaskar, A. D. Chougale, M. J. Kulkarni and A. U. Arvindekar, *Molecular BioSystems*, 2013, **9**, 2463-2472.
45. X. Zhang, L. Li, Z. Xu, Z. Liang, J. Su, J. Huang and B. Li, *PloS one*, 2013, **8**, e59106.
46. B. Bhattacharya, S. Nakka, L. Guruprasad and A. Samanta, *The Journal of Physical Chemistry B*, 2009, **113**, 2143-2150.
47. C. Wa, R. L. Cerny, W. A. Clarke and D. S. Hage, *Clinica Chimica Acta*, 2007, **385**, 48-60.
48. W. Liu, M. A. Cohenford, L. Frost, C. Seneviratne and J. A. Dain, *International journal of nanomedicine*, 2014, **9**, 5461.
49. W. He, Y. Li, C. Xue, Z. Hu, X. Chen and F. Sheng, *Bioorganic & medicinal chemistry*, 2005, **13**, 1837-1845.
50. J. T. Wu, M. C. Tu and P. Zhung, *Journal of clinical laboratory analysis*, 1996, **10**, 21-34.
51. K. Nakajou, H. Watanabe, U. Kragh-Hansen, T. Maruyama and M. Otagiri, *Biochimica et Biophysica Acta (BBA)-General Subjects*, 2003, **1623**, 88-97.
52. P. A. Zunszain, J. Ghuman, T. Komatsu, E. Tsuchida and S. Curry, *BMC Structural biology*, 2003, **3**, 6.

Figure Captions

Figure 1. Chemical structure of 1, 2, 3, 4, 6-penta-*O*-galloyl-*β*-D-glucose (PGG).

Figure 2. MALDI-TOF mass spectra of the +2 ion of: 1) Natural BSA alone, 2) BSA incubated with D-fructose, 3) BSA incubated with D-fructose in the presence of 50 µM PGG, and 4) BSA incubated with D-fructose in the presence of 50 µM aminoguanidine (AG). All samples were prepared in 0.1 M phosphate buffer, pH 7.4 and analyzed after 3 days incubation at 37 °C. The spectrum in each of the profiles indicates the doubly charged BSA (z = 2).

Figure 3. Intrinsic fluorescence profiles of middle stage AGEs: A) Fluorescence time course profiles of reaction mixtures incubated up to 21 days, and B) Percent inhibition of PGG and AG on the formation of AGEs after 7 days incubation. Percentage inhibition was determined on the basis of intrinsic fluorescence readings of each sample relative to that of the control solution set at 100 %. All data points represent the average of triplicate measurements with the bars at each point representing the respective standard deviation (SD).

Figure 4. HPLC-fluorescence profiles of 10 mg/mL BSA and 100 mM D-ribose after 7 days incubation at 37 °C with or without treatments. The excitation and emission wavelengths for detection were set at 360 nm and 430 nm, respectively.

Figure 5. Inhibitory effects of PGG on the final stage of protein glycation in the G.K. peptide-ribose assay. G.K. peptide (40 mg/mL) was co-incubated with ribose (800 mM) for 9 hours in the absence and presence of PGG at concentrations ranging from 1 to 300 µM. Intrinsic fluorescence of each sample was measured at an excitation wavelength of 340 nm and an emission wavelength of 420 nm. Results are means ± SD for three independent tests.

Figure 6. Far-UV circular dichroism (CD) spectra of native BSA (blue), glycated BSA (red), and PGG treated BSA (green).

Figure 7. Far-UV spectrum of Congo red binding assay: native BSA (blue), glycated BSA without any treatment (red), PGG treated BSA (green), and AG treated BSA (purple).

Figure 8. MOE-Docking studies of PGG binding to BSA. Ribbon model of two predicted binding sites (A) and (B). Close up view of binding site 1(C) in subdomain IIIa and binding site 2 (D) in subdomain IIa. Red dash represents hydrogen bonds between PGG and BSA.

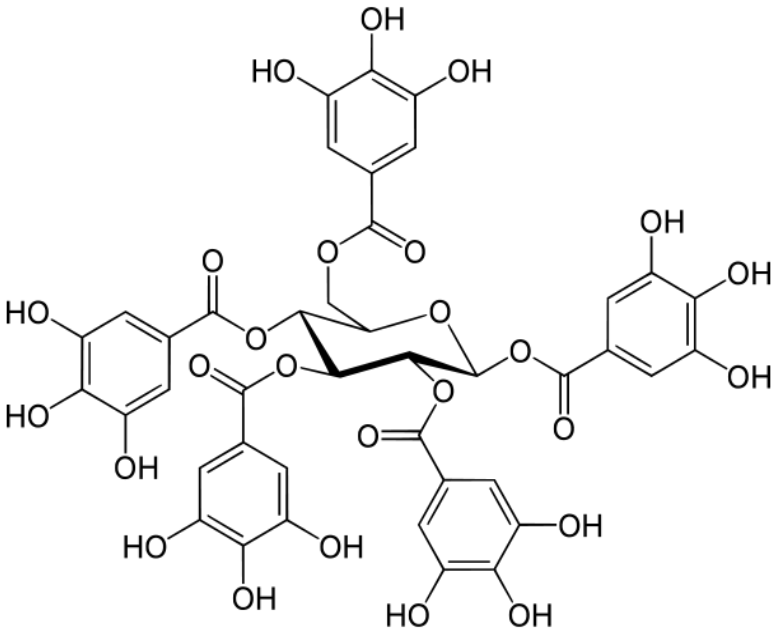

Figure 1. Chemical structure of 1, 2, 3, 4, 6-penta-*O*-galloyl-*β*-D-glucose (PGG).

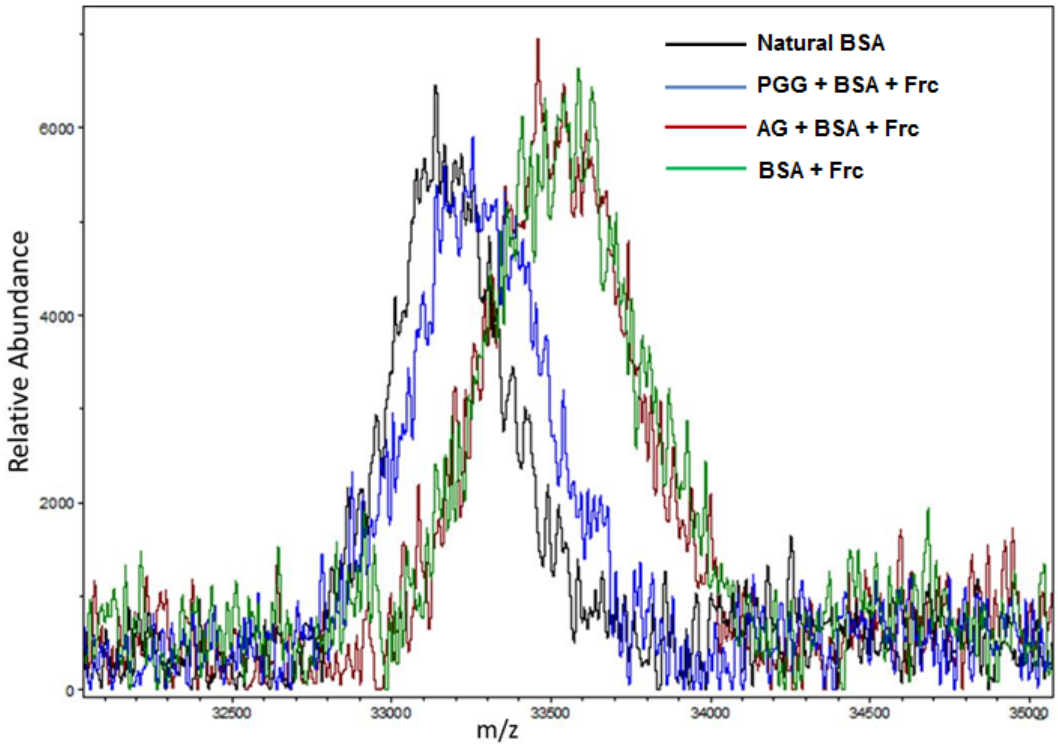

Figure 2. MALDI-TOF mass spectra of the +2 ion of: 1) Natural BSA alone, 2) BSA incubated with D-fructose, 3) BSA incubated with D-fructose in the presence of 50 µM PGG, and 4) BSA incubated with D-fructose in the presence of 50 µM aminoguanidine (AG). All samples were prepared in 0.1 M phosphate buffer, pH 7.4, and analyzed after 3 days incubation at 37 °C. The spectrum in each of the profiles indicates the doubly charged BSA (z = 2).

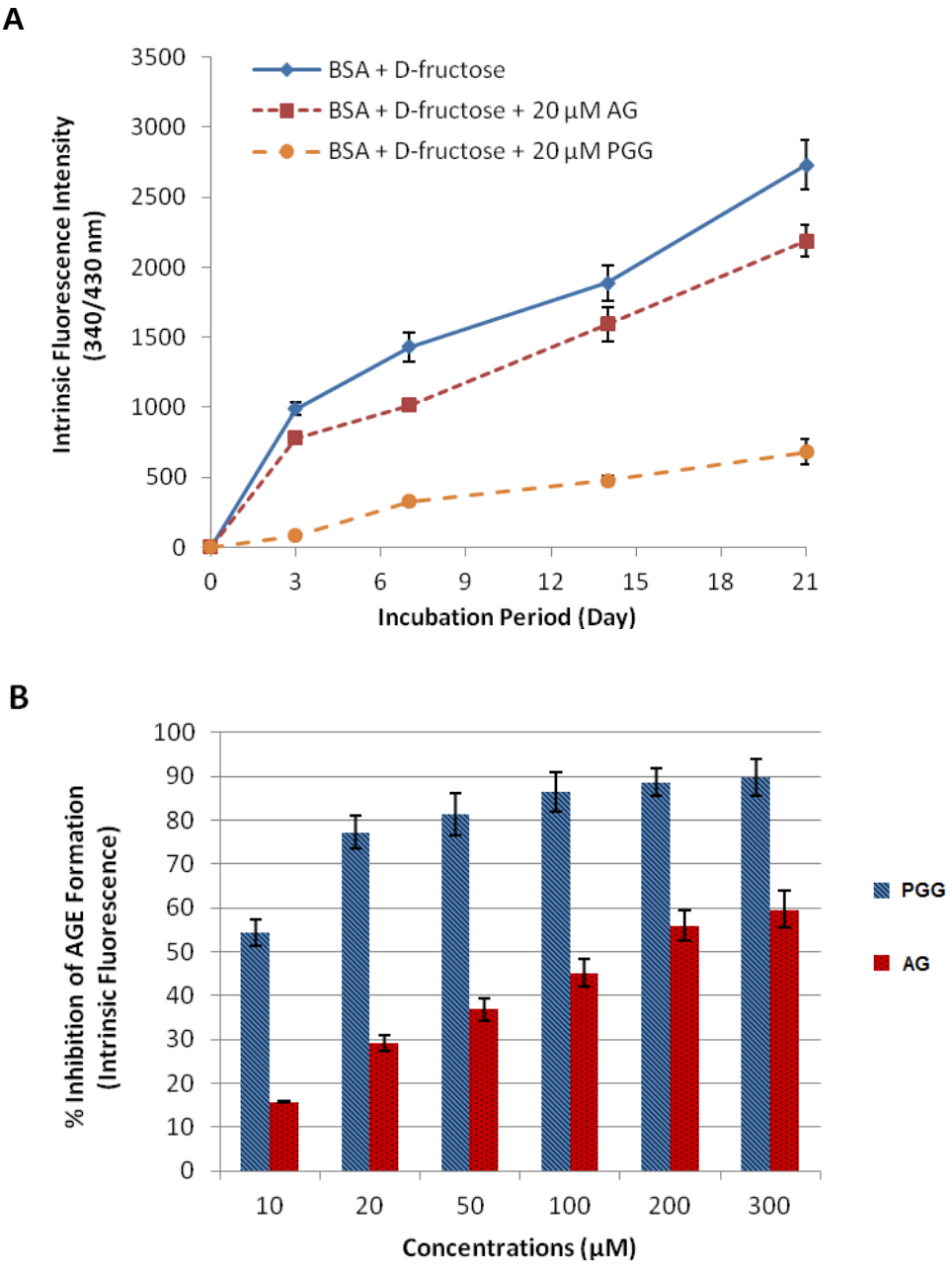

Figure 3. Intrinsic fluorescence profiles of middle stage AGEs: A) Fluorescence time course profiles of reaction mixtures incubated up to 21 days; B) Percentage inhibition of PGG and AG on the formation of AGEs after 7 days incubation. Percentage inhibition was determined on the basis of intrinsic fluorescence reading of each sample relative to that of the control solution set at 100%. All data points represent the average of triplicate measurements with the bars at each point representing the respective standard derivation.

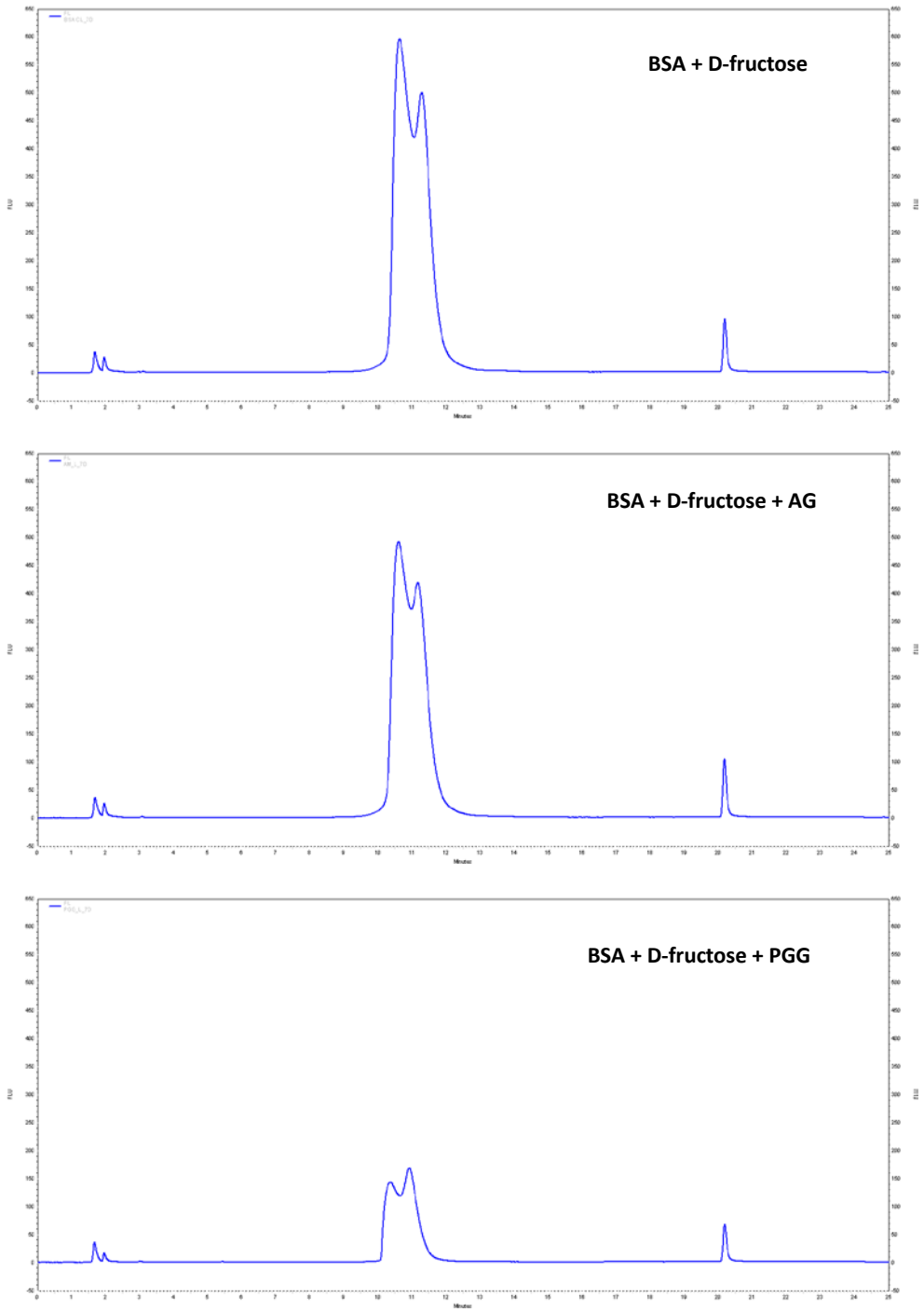

Figure 4. HPLC-fluorescence profiles of 10 mg/mL BSA and 100 mM D-ribose after 7 days incubation at 37 °C with or without treatment. The excitation and emission wavelengths for detection were set at 360 and 430 nm, respectively.

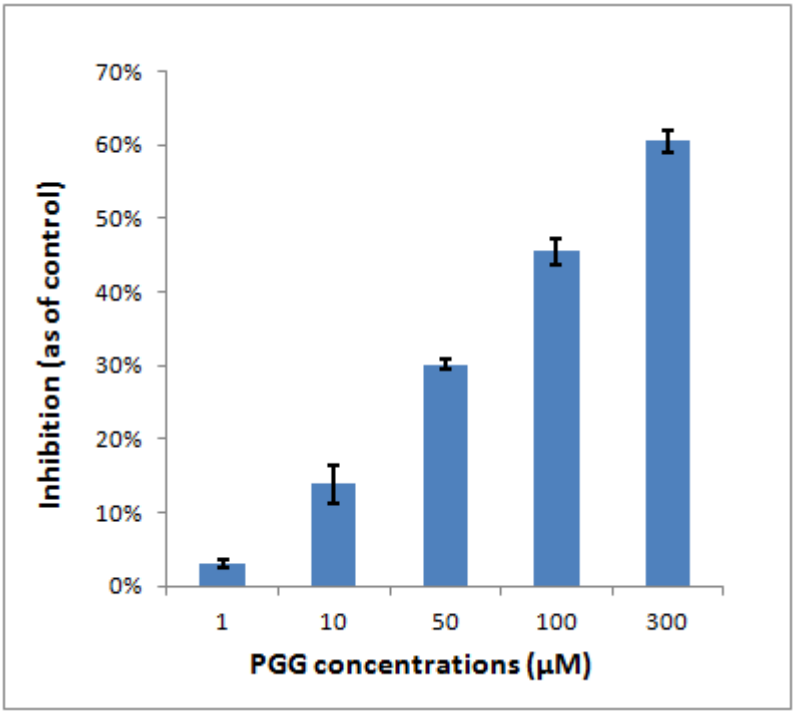

Figure 5. Inhibitory effects of PGG on the final stage of protein glycation in the G.K. peptide-ribose assay. G.K. peptide (40 mg/mL) was co-incubated with ribose (800 mM) for 9 hours in the absence and presence of PGG at concentrations ranging from 1 to 300 µM. Intrinsic fluorescence of each sample was measured at an excitation wavelength of 340 nm and an emission wavelength of 420 nm. Results are means ± SD for three independent tests.

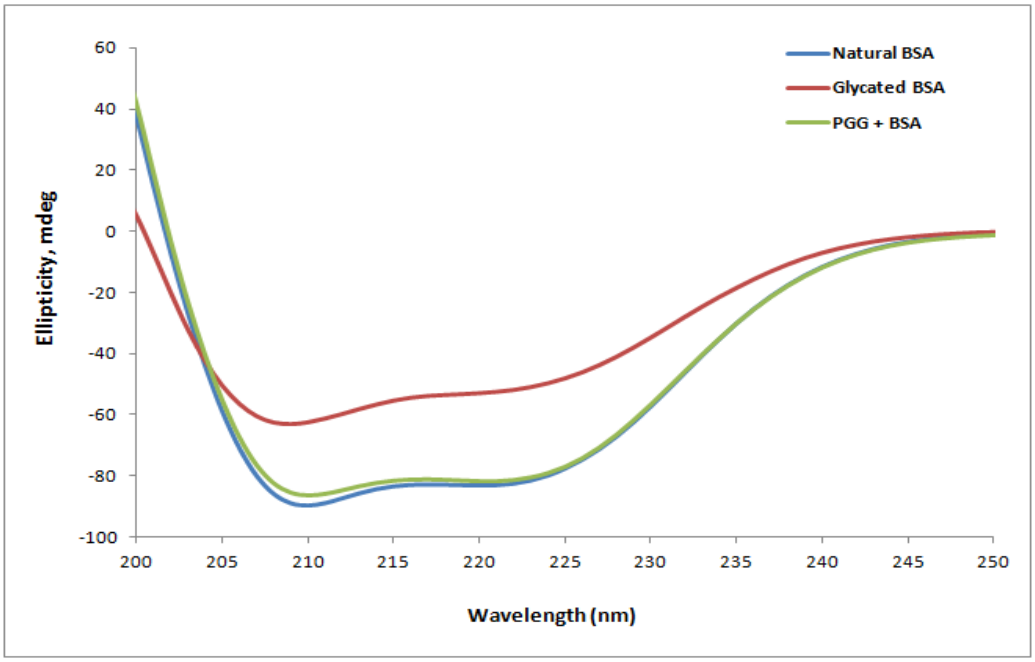

Figure 6. Far-UV circular dichroism spectra of native BSA (blue), glycated BSA (red) and PGG treated BSA (green).

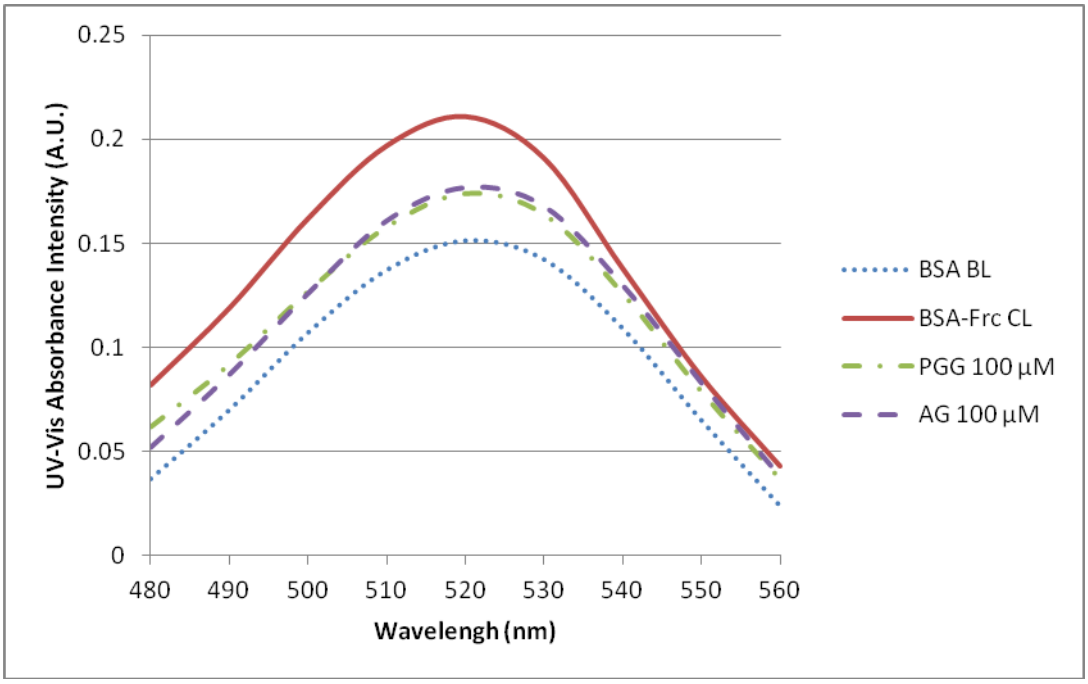

Figure 7. Far-UV spectrum of Congo red binding assay: native BSA (blue), glycated BSA without any treatment (red), PGG treated BSA (green), and AG treated BSA (purple).

A

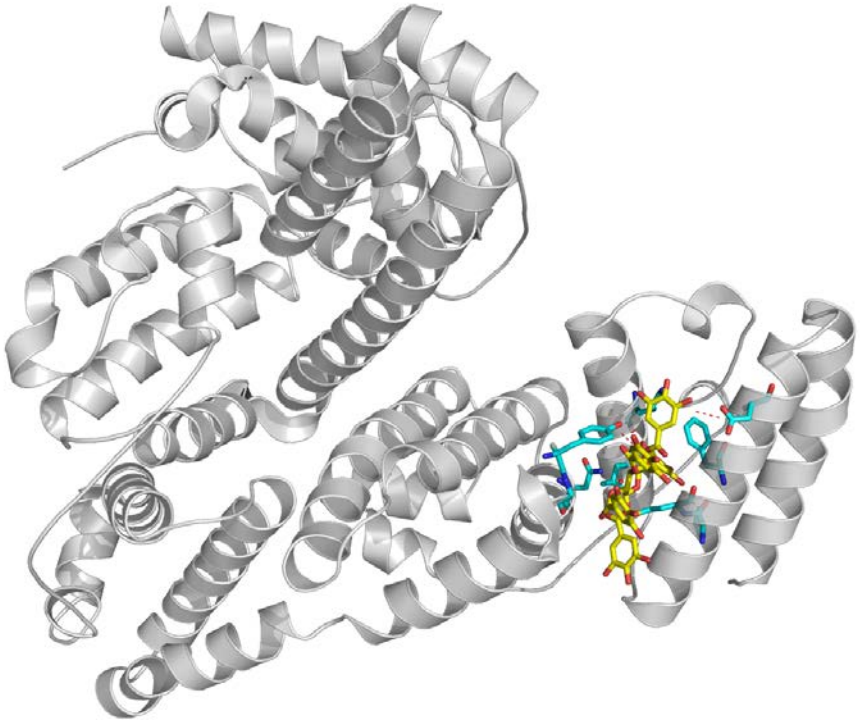

B

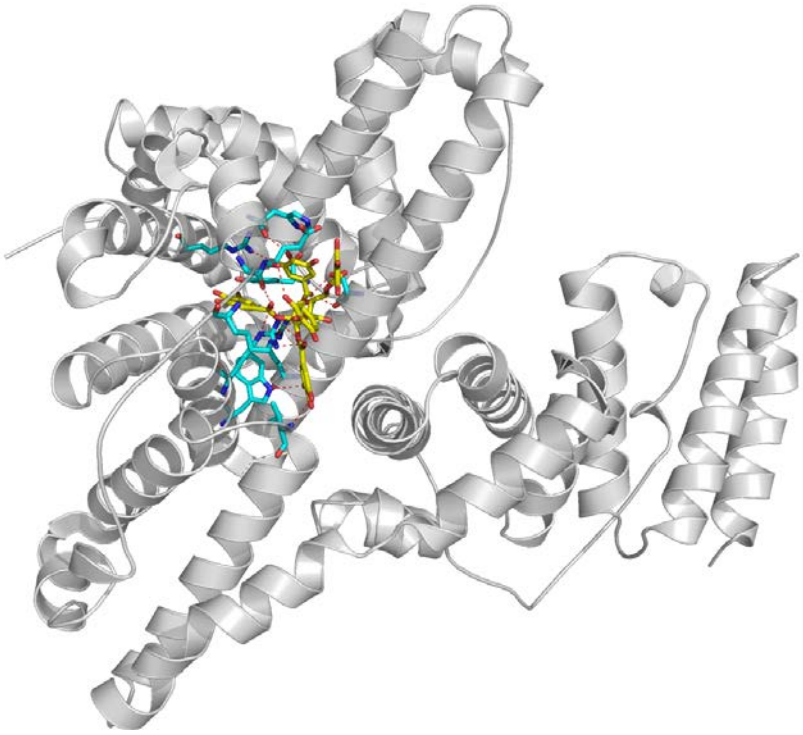

C

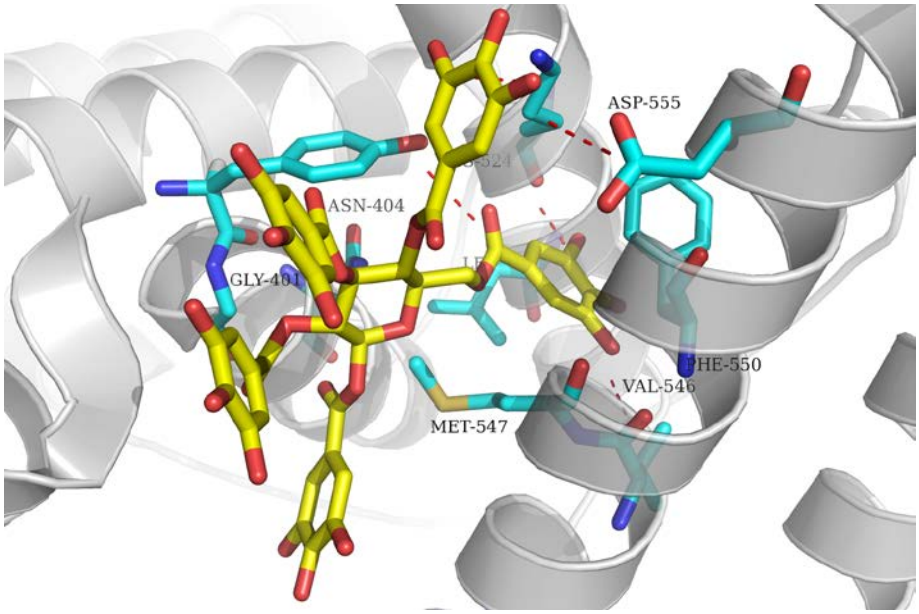

D

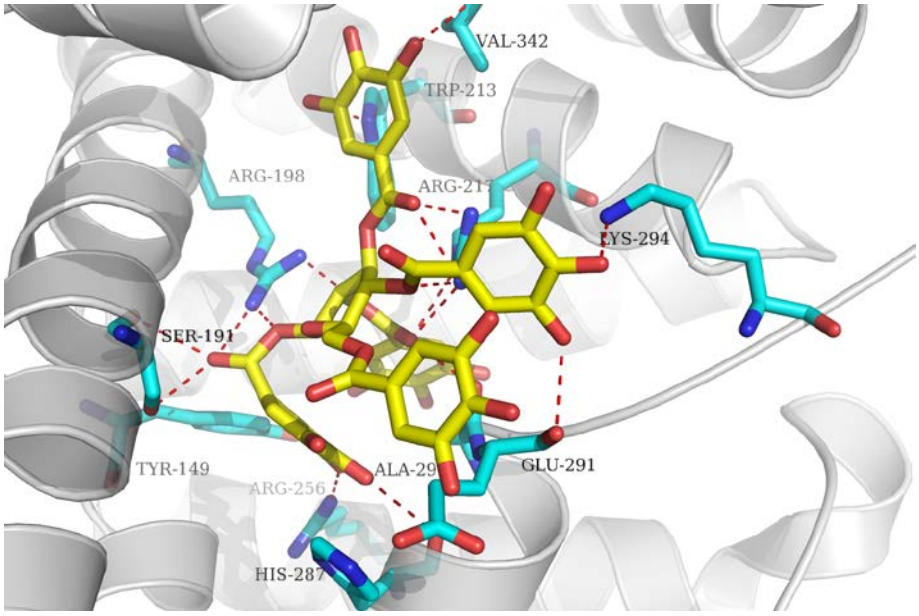

Figure 8. MOE-Docking studies of PGG binding to BSA. Ribbon model of two predicted binding sites (A) and (B). Close up view of binding site 1(C) in subdomain IIIa and binding site 2 (D) in subdomain IIa. Red dash represents hydrogen bonds formed between PGG and BSA.

Table I. CD calculation of Secondary Structure Composition of BSA

Secondary Structure	% Helix	% Strands	Helix (Per 100 Residues)	Strands (Per 100 Residues)
Natural BSA	0.575	0.041	7.127	1.371
Glycated BSA	0.172	0.242	2.263	4.404
50 μM PGG	0.358	0.113	3.943	2.578
50 μM AG*	0.295	0.179	3.52	2.938

* 50 μM Aminoguanidine (AG) served as the positive control.

Table II. Zeta Potential and Electrophoretic Mobility Measurement

	Native BSA	Glycated BSA	PGG (100 μM)	AG (1000 μM)
Zeta Potential ζ (mV)	-8.18 ± 0.35	-106.3 ± 2.82	-30.9 ± 1.27	-28.2 ± 1.06
Electrophoretic Mobility μ ($10^{-9}m^2s^{-1}V^{-1}$)	-0.64 ± 0.03	-8.31 ± 0.22	-2.202 ± 0.10	-2.42 ± 0.08